NuMI Commissioning Report

February 17, 2005

1 Introduction

The Project Execution Plan for the Neutrinos at the Main Injector (NuMI) Project specifies a set of technical goals for project commissioning. In accordance with the Project Execution Plan, these goals must be satisfied for Critical Decision 4 (CD-4), the formal approval to start operations. Table 1.1 summarizes the commissioning goals for NuMI.

Parameter	Measurement	Commissioning Goal
Proton intensity in target hall	Toroid (or equivalent) beam intensity monitor at entrance to the target hall	Greater than 1×10^{12} 120 GeV protons per spill
Beam alignment	Transverse distributions of the proton beam and secondary beams	Proton direction established to within 1 mr of the known direction to the far detector in the Soudan mine
Neutrino beam energy	Near Detector event energy	low energy, 2-4 GeV
Cosmic ray muons detected in the MINOS Near Detector	Near Detector data read out through DAQ system	Majority of the 153 Near Detector planes sensitive to muons
Near Detector neutrino flux	Charged-current event rate in 1.5 ton fiducial region	Observe neutrinos produced in the Near Detector by the NuMI beam
Cosmic ray muons and atmospheric neutrinos detected in each of the two MINOS Far Detector Supermodules	Far Detector data read out through DAQ system	Majority of the 484 planes of the Far Detector sensitive to muons and atmospheric neutrinos

Table 1.1 NuMI technical commissioning goals

The following sections address each of these goals. The section will explicitly describe the measurements that define the successful attainment of the goal and provide documentation that the goal has in fact been attained.

2 Proton Intensity in the Target Hall

The Fermilab Main Injector accelerates protons to a momentum of 120 GeV/c. A set of "kicker" magnets then extracts the 120 GeV protons and sends them into the NuMI beamline, through which they are transported to the NuMI target. The NuMI commissioning goal is to achieve a proton intensity of 1×10^{12} protons per spill at the target.

2.1 Beam Toroids

The intensity of the beam is measured by a series of devices in the Main Injector and in the NuMI beamline. A DC Current Transformer (DCCT) with the device name I:BEAMM in the Main Injector measures the intensity of the Main Injector beam. The primary beam intensity in the NuMI line is measured in two places by bench-calibrated toroid monitors. The first (E:TOR101D) is in the MI60 region, 25 meters downstream of the kicker magnets. The second (E:TORTGTD) is 20 meters upstream of the target. Ensuring that the beam is cleanly extracted from the Main Injector and transported through these monitors checks the calibration. Figure 2.1 shows beam intensity per spill in these three devices from Friday January 22, 20:00 to 20:30 hours. A beam spill occurred every 2 minutes. The intensity ranged from zero to 3×10^{12} protons/spill. Differences in the measurements are due to minor mis-calibration of the NuMI toroids.

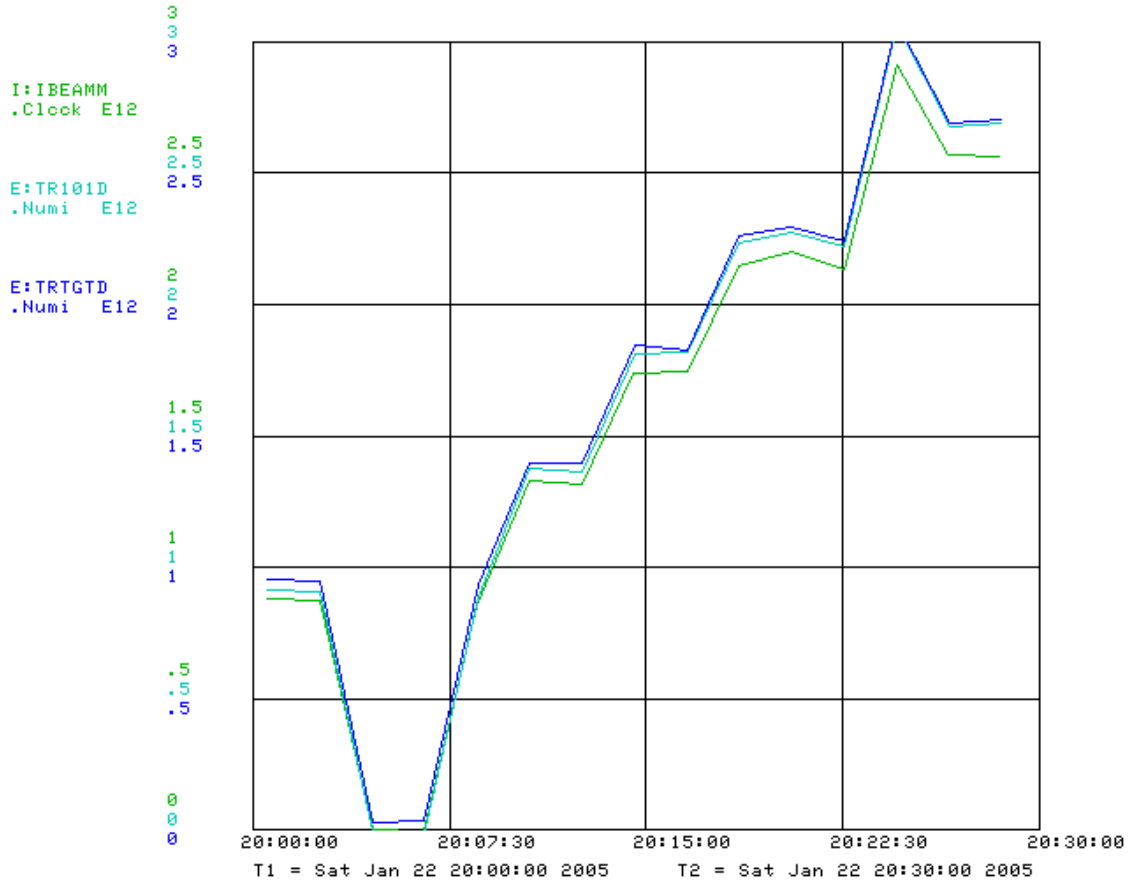

Figure 2.1 Beam intensity in the Main Injector (I:IBEAMM) and in the NuMI beamline (E:TOR101D, E:TORTGTD) for a 30 minute period during the January test run.

Figure 2.2 shows the readout from the downstream toroid in the NuMI beamline during the commissioning run. The vertical scale shows protons on target $\times 10^{12}$. This goal is exceeded throughout most of the run.

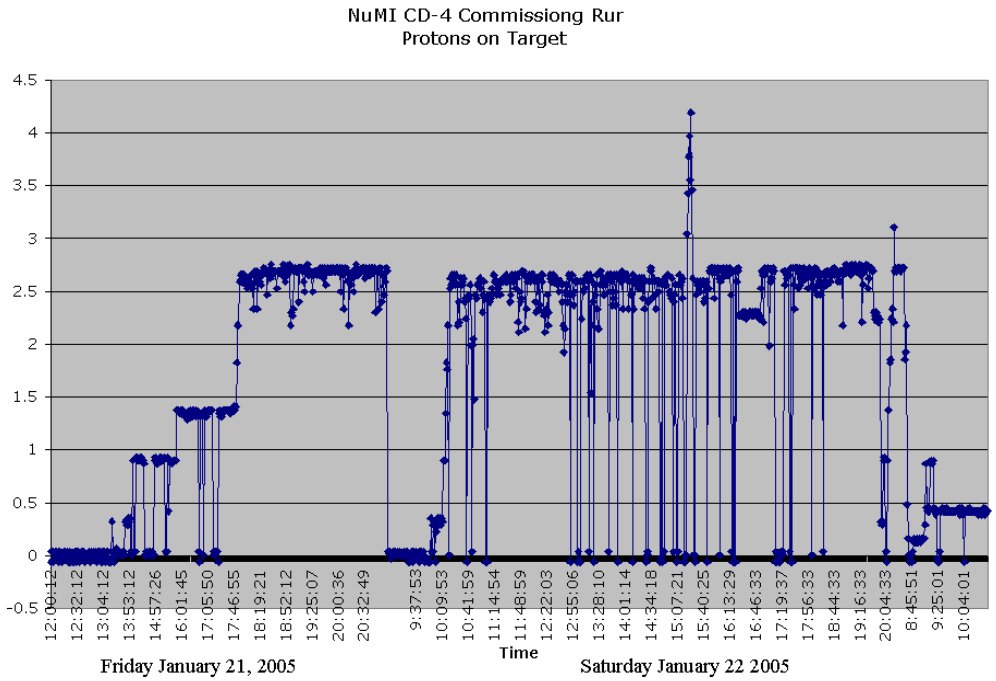

Figure 2.2 Readout from toroid device E:TORTGT during the NuMI commissioning run.

2.2 Summary

The toroid and equivalent devices in the Main Injector and the NuMI beamline have measured beam intensities during the NuMI commissioning run. The proton intensity exceeds the commissioning goal of 1×10^{12} protons per spill at 120 GeV.

3 Beam Alignment

The commissioning goal for alignment of the NuMI beam is to establish the direction of the primary proton beam to within 1 milliradian (mr) of the known direction to the MINOS far detector in the Soudan mine. Measurements with the Global Positioning System (GPS) locate a network of survey monuments on the surface of the Earth. The Fermilab alignment group extended this network below ground at both sites, installing survey monuments in the Pre-target, Target, and Absorber Hall regions and at Soudan. Quality Assurance measurements taken during the NuMI tunnel construction have shown the tunnel to be aimed at the mine to within 0.015 mr. To meet the commissioning goal, the NuMI proton beam must be aligned with the NuMI tunnel to within an acceptable tolerance.

A set of beam profile monitors in the NuMI pre-target area measures the proton beam position as it enters the target hall. These monitors are aligned relative to the NuMI survey monuments. The aiming of the proton beam is measured by the distributions in monitors for the primary and secondary beams. Hadron monitor measurements provide the most direct measure of the proton beam alignment. Muon monitor measurements provide additional confirmation.

3.1 Beam Profile Monitors

The beam profile is monitored by segmented foil Secondary Emission Monitors (SEMs), which measure the horizontal or vertical position of the beam with a precision of 50 μm or better. The SEMs are aligned relative to the NuMI facility survey monuments. Figure 3.1 shows the readout from the SEM profile monitors as measured during the NuMI commissioning run on January 21, 2005. They show clean extraction and transport of protons through the NuMI beamline with the beam centered at the entrance to the target hall.

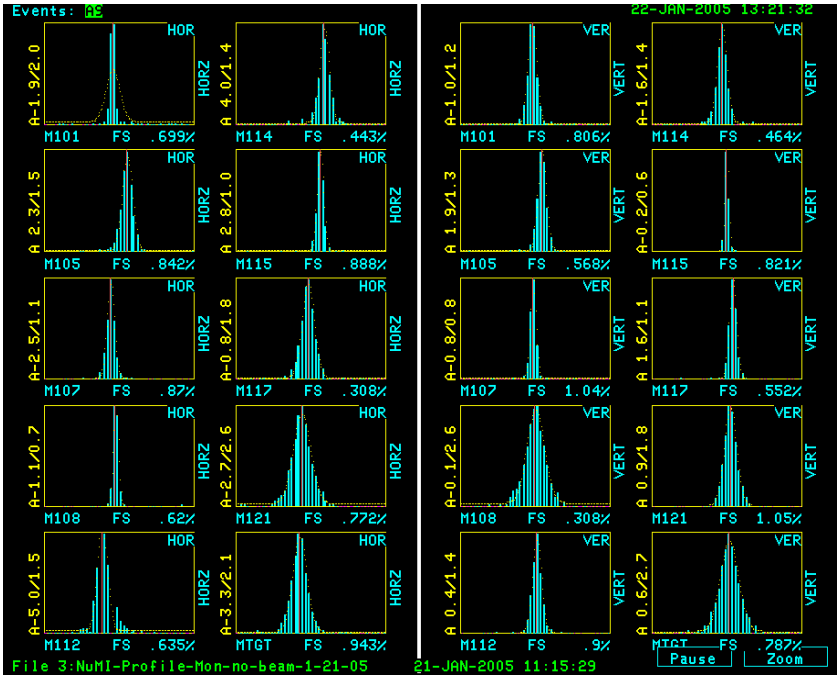

Figure 3.1 SEM readouts from the NuMI beam commissioning run.

3.2 The NuMI Hadron Monitor

The NuMI hadron monitor is a 7 × 7 array of parallel plate ionization chambers, which is installed in the absorber stack between the downstream end of the decay pipe and the upstream face aluminum absorber core. The hadron monitor is designed to verify the alignment of the NuMI proton beam. It is located 732.1 m downstream of the pre-target SEMs and is aligned relative to the Absorber Hall survey monuments. The initial beam

pulses were directed into the NuMI beamline, with no target in place, the horns de-energized, and the decay pipe evacuated, thus leaving as clear a path as possible for the primary beam protons to reach the monitor. The relative count rates in the ionization chamber plates show the positioning of the NuMI proton beam.

3.2.1 Calibration and Alignment of the Hadron Monitor

The relative pixel calibration was established to within 3% using radioactive sources, with the initial variation at the 10% level before correction. The hadron monitor is installed in the absorber stack through a 6-inch slot and is positioned on a set of support rails. The rails were installed and surveyed relative to the Absorber cavern alignment network prior to the construction of the hadron absorber core. Measurements of the installed hadron monitor show that the nominal beam center is aligned with the center ionization chamber.

3.2.2 Beam Position at the Hadron Monitor

Figure 3.2 and Figure 3.3 depict the readout from the NuMI hadron monitor during the commissioning run in horizontal and vertical views. The horizontal axes of the figures show the position, in inches, of the individual ion chambers. The horizontal axis represents the charge readout during the beam pulse. The distance from the MTGT monitor to the hadron monitor is 732.1 m. Pulse-to-pulse measurements in the SEMs and the hadron monitor have verified the accuracy of the proton beam angle within the tunnel to .035 mr.

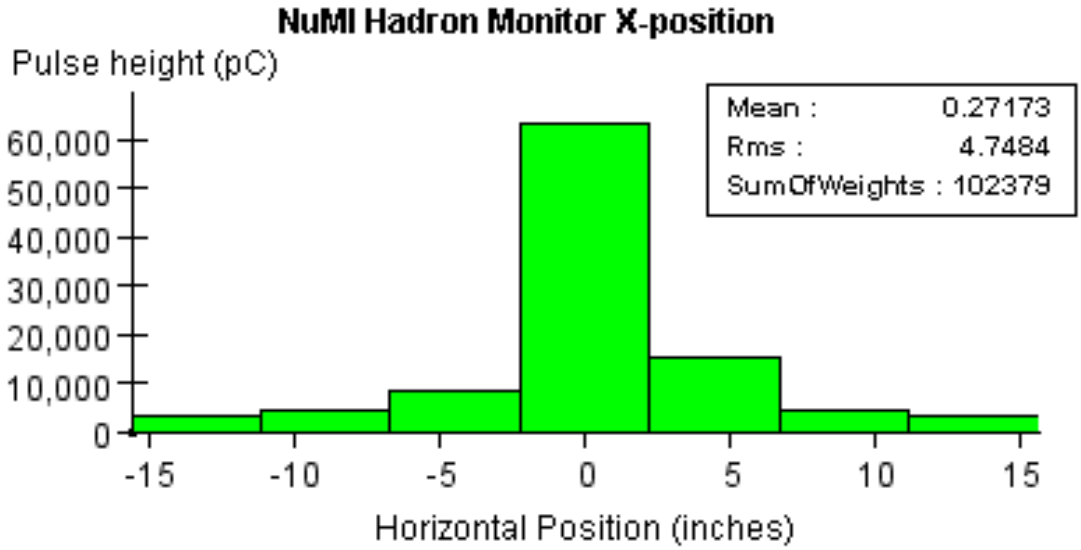

Figure 3.2 *x*-position of hadron monitor readout from beam commissioning.

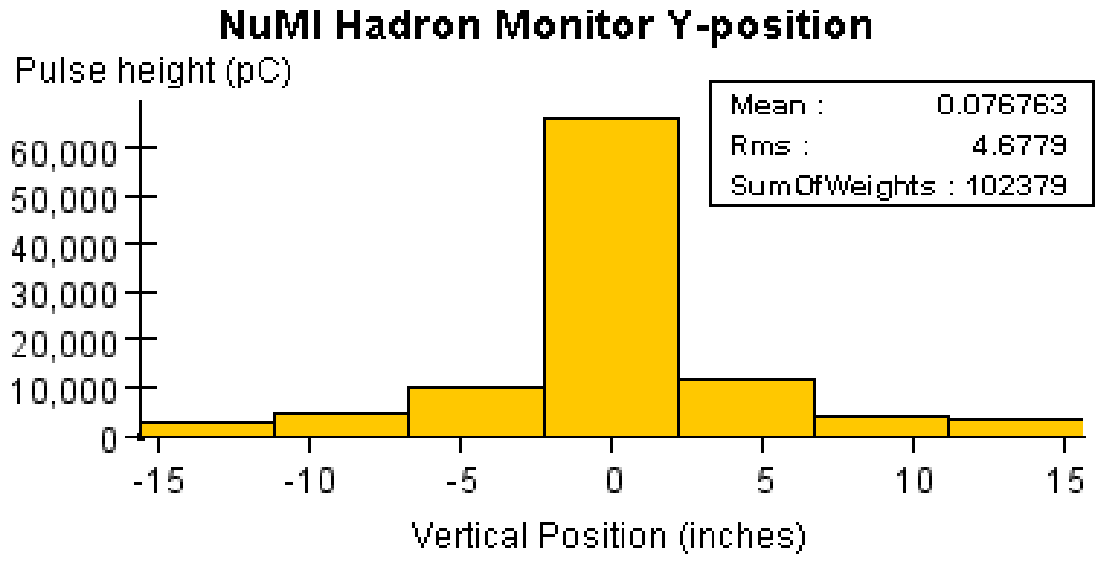

Figure 3.3 *y*-position of hadron monitor readout from beam commissioning.

3.3 The NuMI Muon Monitors

The NuMI muon monitors comprise three sets of 9×9 arrays of ion chambers, each array covering 2m × 2m. These devices, named E:MMA1D, E:MMA2D and E:MMA3D in ACNET, are located in the first, second and third muon alcoves downstream of the hadron absorber. Their function is to monitor the NuMI beam by measuring the position and relative intensity of the muon flux as it passes through successive amounts of material.

The commissioning run included a target scan with the beam, during which the muon monitors read out data as the beam moved from the target center to the baffle. The baffle is 2.5 meters upstream of the target, so that when the proton beam strikes the baffle, the horns focus a higher-energy spectrum of pions than when the beam hits the target. The focusing of higher-energy pions results in a higher-energy spectrum of muons. The energy that a muon requires to penetrate the rock to reach the first, second and third muon alcoves is approximately 4 GeV, 9 GeV and 17 GeV, respectively. Figure 3.4 and Figure 3.5 demonstrate the ability to aim and align the NuMI beam. Figure 3.4 shows the horizontal and vertical projections of the three muon monitors superimposed when the proton beam is centered on the target. The distribution is centered, with relatively low readings in the two downstream monitors. In Figure 3.5, the proton beam is deliberately striking the baffle. The distribution is off-center, reflecting the fact that the beam is not on target. The number of muons reaching alcoves 2 and 3, relative to those in alcove 1, is significantly higher, indicating a higher-energy muon spectrum as expected.

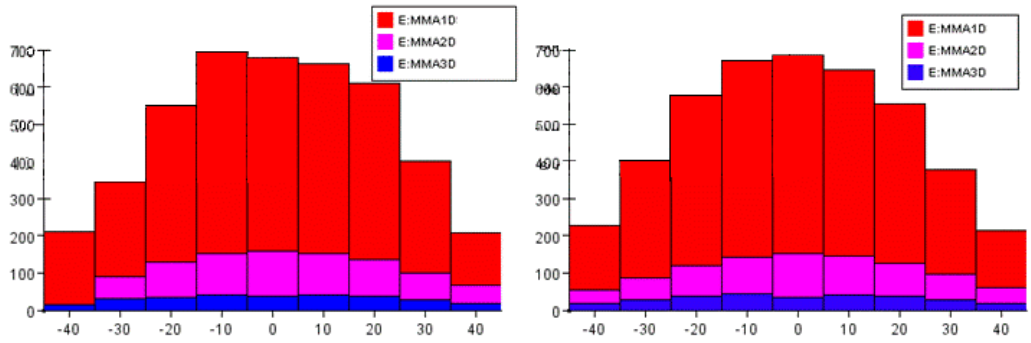

Figure 3.4 Muon monitor readout during the NuMI commissioning run with the beam focused on target. The left histogram shows x position in inches; the right histogram shows *y* position in inches.

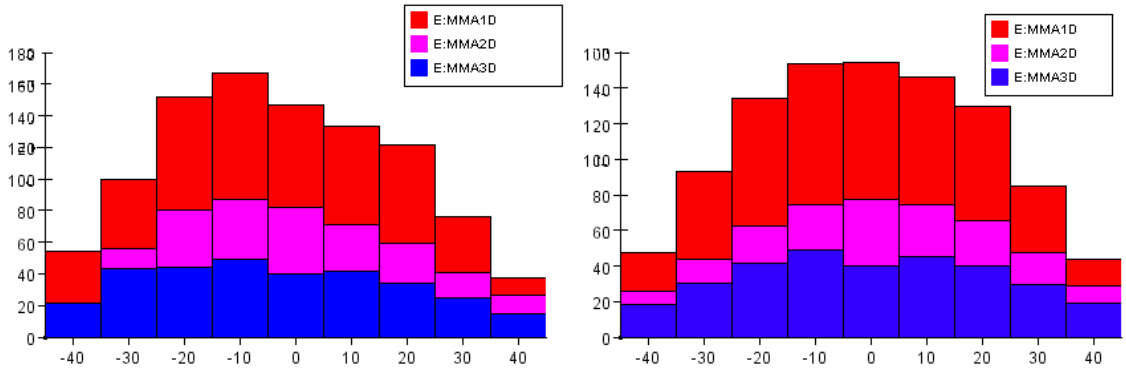

Figure 3.5 Muon monitor readout during the NuMI commissioning run with the beam deliberately focused on the baffle. The left histogram shows x position in inches; the right histogram shows *y* position in inches.

3.4 Summary

Data from the commissioning run show the primary and secondary beam monitors to perform well. Combining the errors of the NuMI tunnel alignment with the Soudan mine (.015 mr) and the proton beam with the NuMI tunnel (.035 mr), we find that the proton beam is aligned with the Soudan mine to within .038 mr, well within the commissioning goal. Thus, this commissioning goal has been achieved.

4 Cosmic Ray Muons in the MINOS Near Detector

The installation of the MINOS Near Detector began in March 2004 and was completed in August 2004. Initial testing of the Near Detector Electronics and DAQ system took place during this time, using natural radioactivity and dark current from the phototubes. As the construction progressed, the detector planes were used to reconstruct muon tracks from cosmic rays and the completed detector now has a substantial sample of cosmic ray data. The commissioning goal requires that the majority of the 153 active planes in the Near

Detector be sensitive to muons. Data read out through the near detector Data Acquisition (DAQ) system are used here to demonstrate that this has been achieved.

4.1 Near Detector Plane Sensitivity

Figure 4.1 depicts the arrangement of scintillator planes in the two sections of the Near Detector. In the calorimeter section all steel planes are covered by scintillator; every fifth is fully covered, while the intervening planes are partially covered. In the spectrometer section every fifth steel plane is fully covered by scintillator, while the intervening planes are uninstrumented steel. This configuration dictates the way in which events in the Near Detector are triggered.

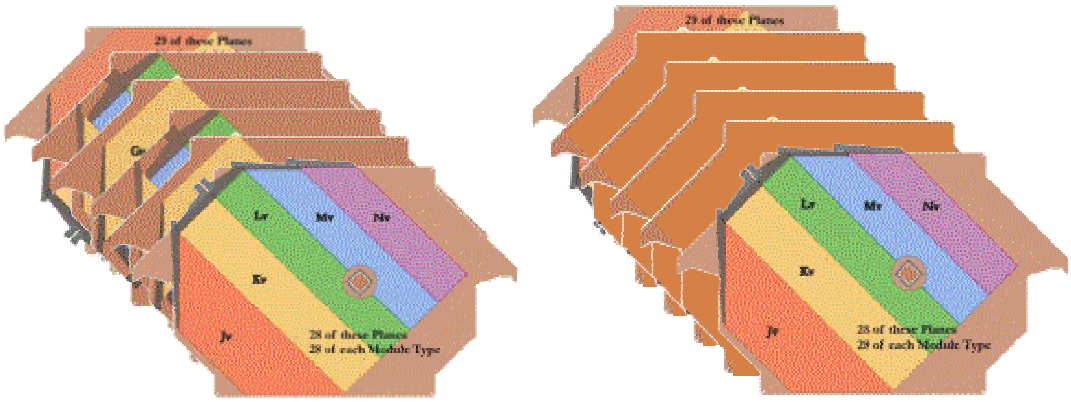

Figure 4.1 Schematic illustration of the calorimeter (left) and spectrometer (right) planes of the MINOS Near Detector.

4.1.1 Near Detector Trigger

All of the data presented in this section were recorded with the "10/12" trigger or the "10 activity" trigger. The "10/12" trigger reads out the detector when 10 out of 12 consecutive planes register a "hit". The "10 activity" trigger reads out the detector when 10 detector planes anywhere register a "hit". By focusing on events that extend over 10 or more planes, these triggers target the penetrating muons.

4.1.2 Near Detector Plane Occupancy

Figure 4.2 and Figure 4.3 show a pair of occupancy plots for the reconstructed cosmic muons in the MINOS Near Detector. The color gradations indicate the number of reconstructed muon tracks passing through each module or strip for a selected set of data runs. Figure 4.2 depicts the number of reconstructed tracks that pass through each scintillator module. Figure 4.3 depicts the number of reconstructed tracks that pass through each scintillator strip. The occupancy plots show that not only are all of detector planes functioning, but all of the modules and most of the scintillator strips are functioning as well. The densely-occupied region at the lower left is the fiducial region of the calorimeter section, including fully- and partially-instrumented planes. The vertical lines extending above this region represent the additional modules of the fully-

instrumented planes (one in every five). The right-hand side of the plot represents the spectrometer region.

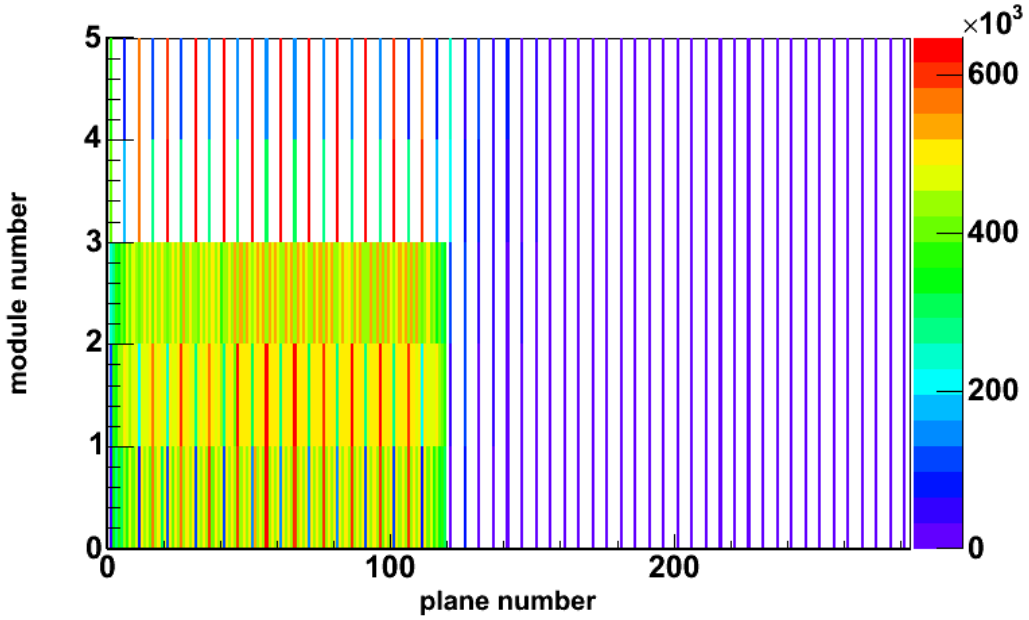

Figure 4.2 Cosmic ray muon occupancy (module *vs.* plane) for the MINOS Near Detector.

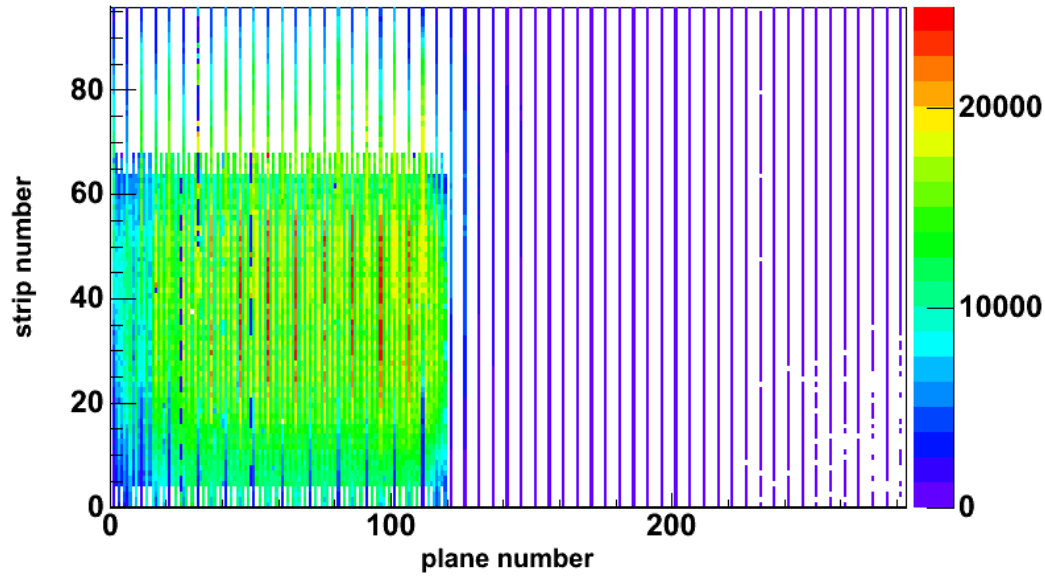

Figure 4.3 Cosmic ray muon occupancy (strip *vs.* plane) for the MINOS Near Detector.

These plots verify that the detector, electronics, DAQ and reconstruction software are functioning and that all active planes are sensitive to muons. The downstream spectrometer region is sparsely occupied; that is expected and understood. The spectrometer region has a 4-fold plex, namely 4 different scintillator strips are read out by

the same electronics channel. This results in four "mirror" images in each view of the spectrometer that cannot by themselves reconstruct the actual event. Thus the reconstruction software reconstructs 3-dimensional tracks only if they start in the calorimeter region, which is not multiplexed. The Near Detector is, of course, not optimized to detect nearly-vertical cosmic rays. Muon tracks from beam neutrinos lie closer to the detector axis and, in general, are easier to follow from the calorimeter into the spectrometer.

4.2 Cosmic Ray Muon Distributions

Figure 4.4 depicts the event display for a typical cosmic ray muon in the MINOS Near Detector. The top panel shows the transverse position of hit strips in the *u* view versus the *z* position of the plane. The middle panel shows the same for the *v* view. The relative sizes of the signal from each hit in the event are shown in the histograms along the top and sides of the *uz* and *vz* views. The lower left panel is the *xy* projection of the track. The lower right graph shows the time for each digit along the track versus its y-position.

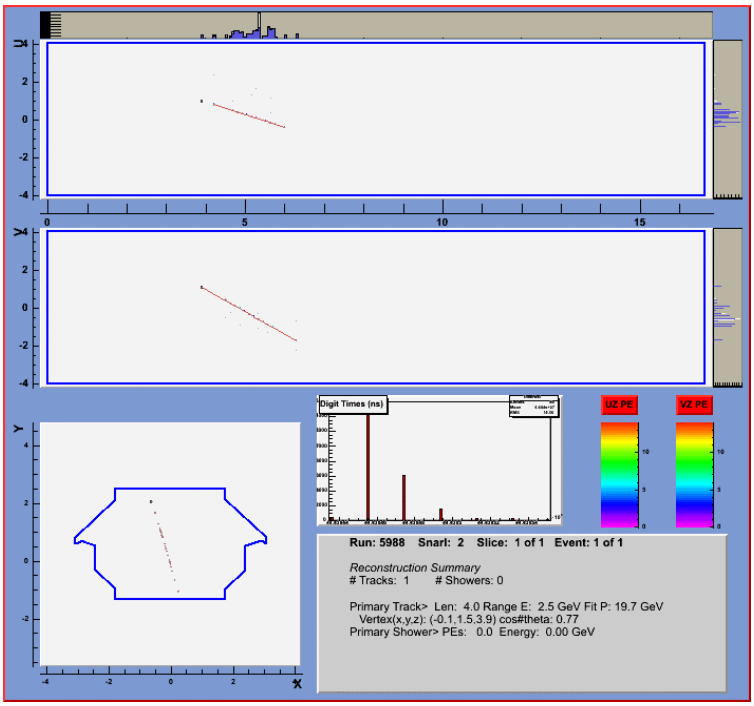

Figure 4.4 Event display of a typical cosmic ray muon in the Near Detector.

Figure 4.5 shows the zenith angle distribution of cosmic ray data for tracks with a length greater than 20 planes. The probability that these tracks are muons, as opposed to detector noise, is extremely high. The zenith angle distribution is in agreement with expectations: very few horizontal muons and none from directly above. The latter effect is due to the software trigger used to record these events and the track length criterion.

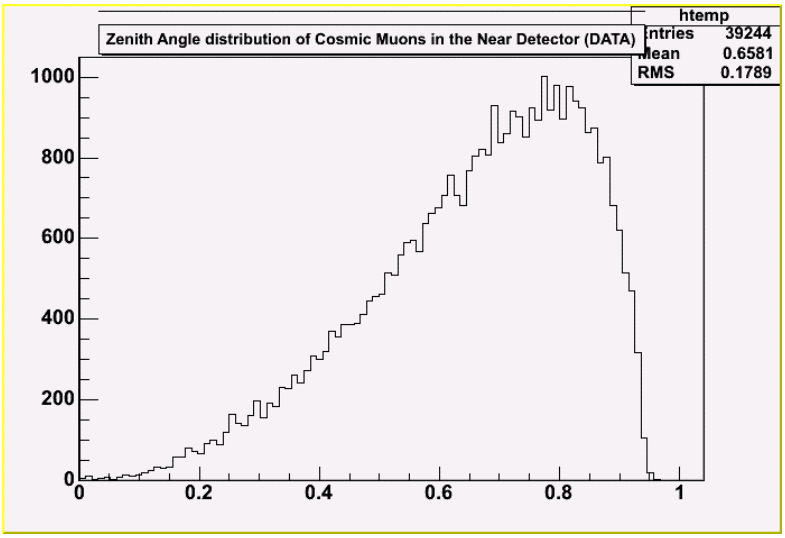

Figure 4.5 Zenith angle distribution of cosmic ray muons in the near detector.

The azimuth angle distribution again reflects the trigger used and the detector geometry: Muons traversing the detector along the *x* direction won't satisfy the trigger criterion. Again the results agree very well with expectations.

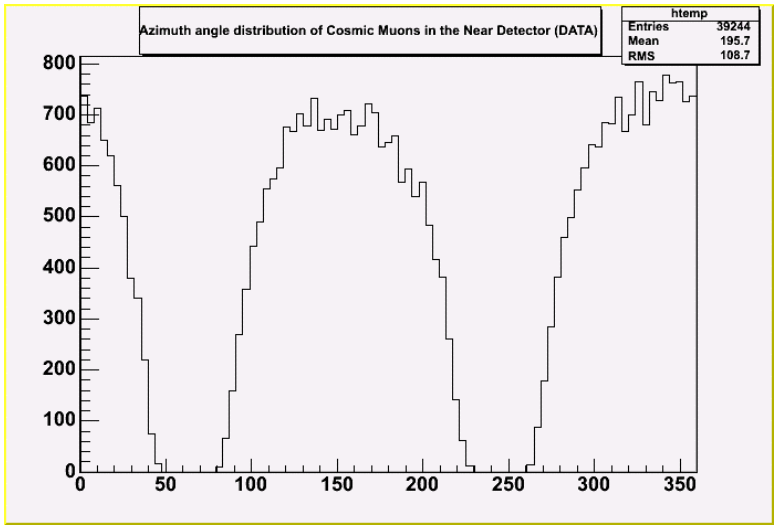

Figure 4.6 Azimuthal distribution of cosmic ray muons in the near detector.

4.3 Summary

The data presented in this section demonstrate that the MINOS Near Detector is capable of observing cosmic ray muon events and reading them out through the MINOS DAQ system. They also show that all of the detector's active planes are sensitive to muons. Thus, this commissioning goal has been achieved.

5 Cosmic Ray Muons & Atmospheric Neutrinos in the MINOS Far Detector

The MINOS far detector has taken cosmic ray data since September 2002, when the first supermodule was completed and magnetized. Construction of the second supermodule was still in progress and was completed in July 2003. The full magnetized detector has taken data since that time. The far detector routinely observes muons produced by cosmic ray interactions in the atmosphere. The commissioning goal requires that the majority of the Far Detector's 484 planes are sensitive to muons and atmospheric neutrinos.

Muons and neutrino events are observed in both supermodules of the Far Detector. Data read out through the Far Detector DAQ system is used to reconstruct these events, which include cosmic ray muons and neutrinos. The latter are observed in both upward-going muon events and contained events.

5.1 Far Detector Plane Sensitivity

Each instrumented plane of the Far Detector contains 8 scintillator modules. Each module contains 192 scintillator strips.

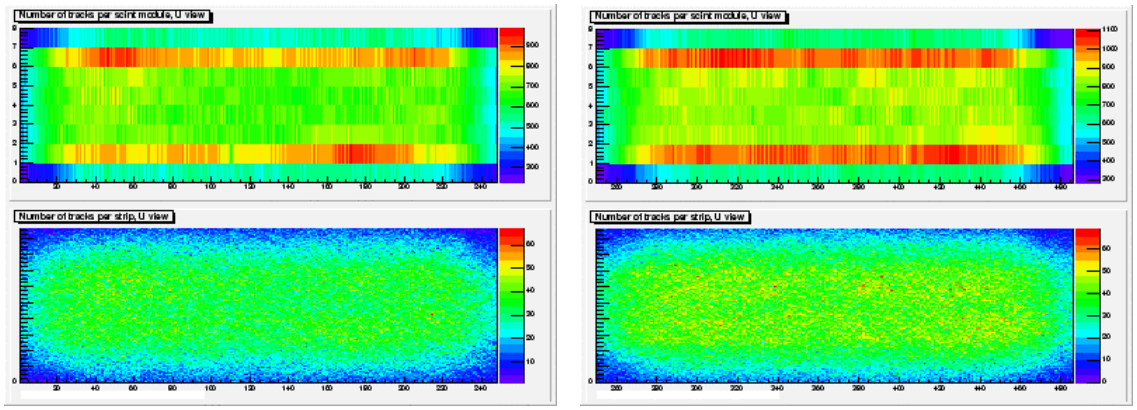

Figure 5.1 Occupancy plots from muon tracks in the MINOS far detector.

Figure 5.1 shows the occupancy of tracks by module and by strip for both supermodules of the far detector. The two plots on the left are for supermodule 1; those on the right are for supermodule 2. The horizontal axis on all plots represents plane number. On the upper plots, the vertical axis represents the scintillator module number. On the lower plots, the vertical axis represents the scintillator strip number. The color gradations indicate the number of reconstructed muon tracks passing through each module or strip for a selected set of data runs. The red bands in the upper plots represent the largest modules (2 and 7), which have the greatest number of tracks, while the smallest modules (1 and 8), have the fewest. This result is just as one would expect. These plots not only demonstrate that all of the instrumented Far Detector planes are sensitive to muons, but also that all of the modules and most of the strips are sensitive to them as well.

5.2 Observation of Muons

Figure 5.2 and Figure 5.3 show the geometrical distribution of observed muons. The criteria for identifying an event as containing a muon require that a reconstructed track traverse at least 20 planes in the detector and that the track length be at least 2 meters.

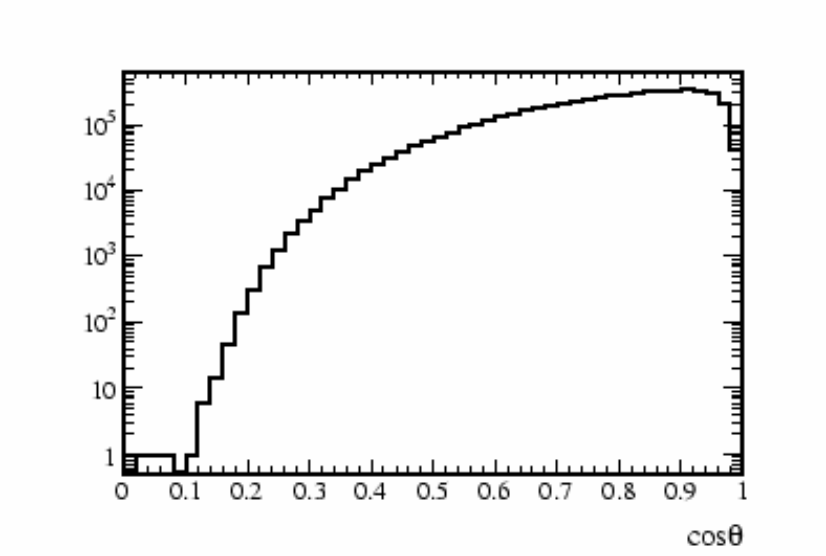

Figure 5.2 Zenith angle distribution of cosmic ray muons in the MINOS far detector.

Figure 5.2 shows the zenith angle [cos(θ)] distribution. The sharp drop off of the distribution near cos(θ) = 1 reflects the fact that the muons coming from directly above the detector will not pass the cuts on the number of planes crossed and track length, due to low acceptance for those angles. The distribution also falls with increasing zenith angle, as the amount of rock between the detector and the surface increases rapidly for values of cos(θ) near the horizon. Only the most energetic muons can penetrate the overburden at these angles.

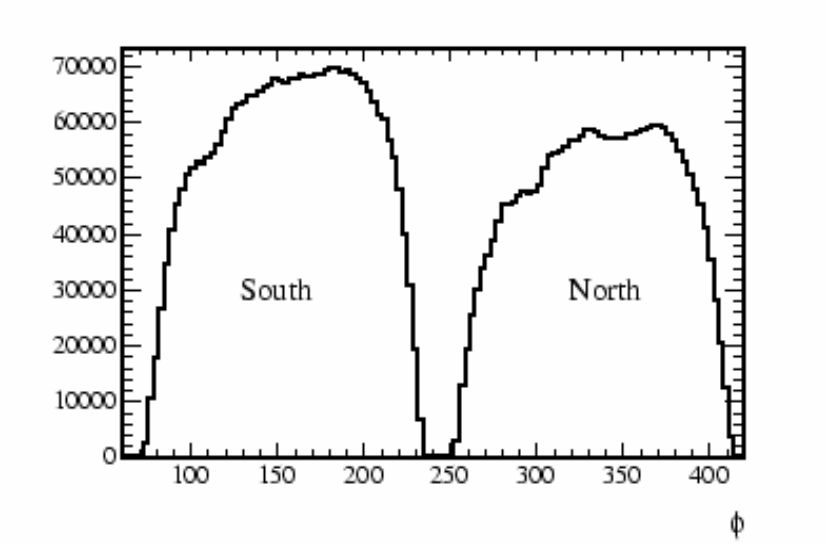

Figure 5.3 Azimuthal distribution of cosmic ray muons in the MINOS far detector.

Figure 5.3 shows the azimuthal distribution of the cosmic ray muons. The azimuthal angle is defined by $\varphi = 0°$ due north and $\varphi = 90°$ due east. Since the detector is not aligned north-south, but rather on a line pointing toward Fermilab, the muons with values of $\varphi < 60°$ have had 360° added to the azimuth for this plot. This is to make the muons from the north be in a contiguous region, $240° < \varphi < 420°$. Similarly, muons coming from the south have $60° < \varphi < 240°$. More muons come from the south than the north because there is more rock to the north.

5.3 Upward-Going Muons from Atmospheric Neutrinos

The far detector has observed muons produced by neutrino interactions in the rock surrounding the detector. These muons are uniquely identifiable when they come from below the detector, where the amount of rock between the detector and the surface is so great that cosmic ray muons cannot penetrate it. MINOS is able to observe neutrino-induced muons coming from zenith angles $-1 < \cos(\theta) < 0.1$ (the flat overburden at the Soudan site allows neutrino-induced muons coming from above the horizon to be observed).

5.3.1 Detector Timing Calibration

A good timing calibration is essential for identifying neutrino-induced muons coming from below the horizon, as these events are selected based on the timing of the hits along the tracks. The $1/\beta$ distribution of the muons, where β is the ratio of the measured muon velocity to the speed of light, provides a quality check of the timing calibration.

Figure 5.4 shows the $1/\beta$ distribution for events satisfying the muon selection criteria. The downward-going muons have $1/\beta \sim 1$ and upward-going candidates have $1/\beta \sim -1$. Gaussian distributions fitted to the upward- and downward-going muons have widths of 0.05, indicating timing calibrations that are more than adequate to distinguish upward- from downward-going muons.

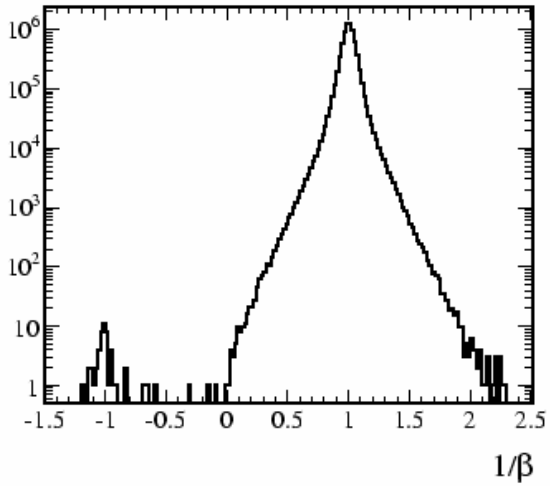

Figure 5.4 Timing distributions ($1/\beta$) for muons in the MINOS far detector.

5.3.2 Observation of Upward-Going Muons

The magnetic field in the far detector allows the charge sign of the particles interacting in it to be determined. Figure 5.5 shows the event display for an upward going μ^+. The top panel shows the transverse position of hit strips in the *u* view versus the *z* position of the plane for both supermodules. The middle panel shows the same for the *v* view. The relative sizes of the signal from each hit in the event are shown in the histograms along the top and sides of the *uz* and *vz* views. The lower left panel is the *xy* projection of the track. The lower right graph shows the time for each digit along the track versus its *y*-position, as the *y* direction increases away from the center of the Earth. This muon is clearly upward-going since the time of the hits along the track increase with increasing values of *y*. The lower right hand legend gives a summary of the event information.

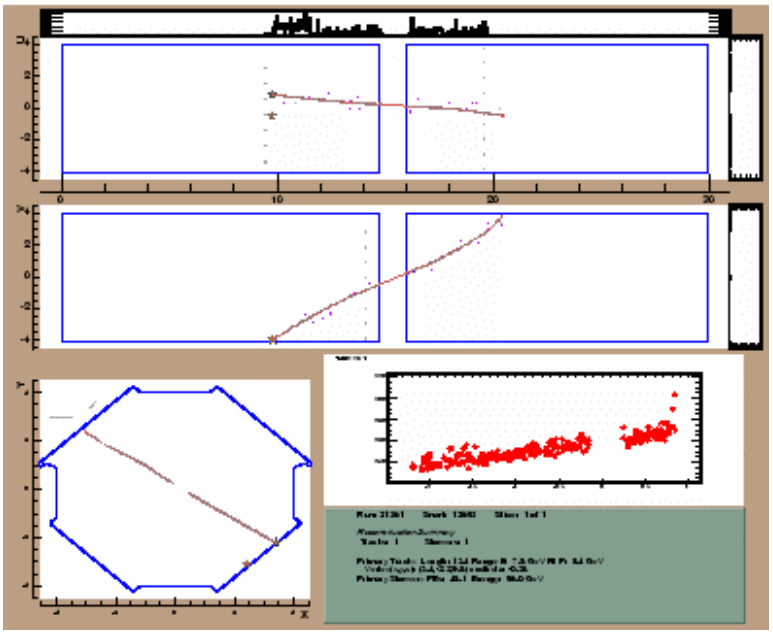

Figure 5.5 Event display for an upward-going muon in the MINOS far detector.

5.4 Contained Neutrino Events

As the name implies, a fully-contained event is one in which the charged particles observed do not enter or exit the detector. This is an indicator that they have been produced by a neutrino interaction at the endpoint of the event. Figure 5.6 and Figure 5.7 show sample events of this type. These were chosen from a set of 37 candidate events derived from 2.52 kiloton-years of cosmic ray data in the far detector.

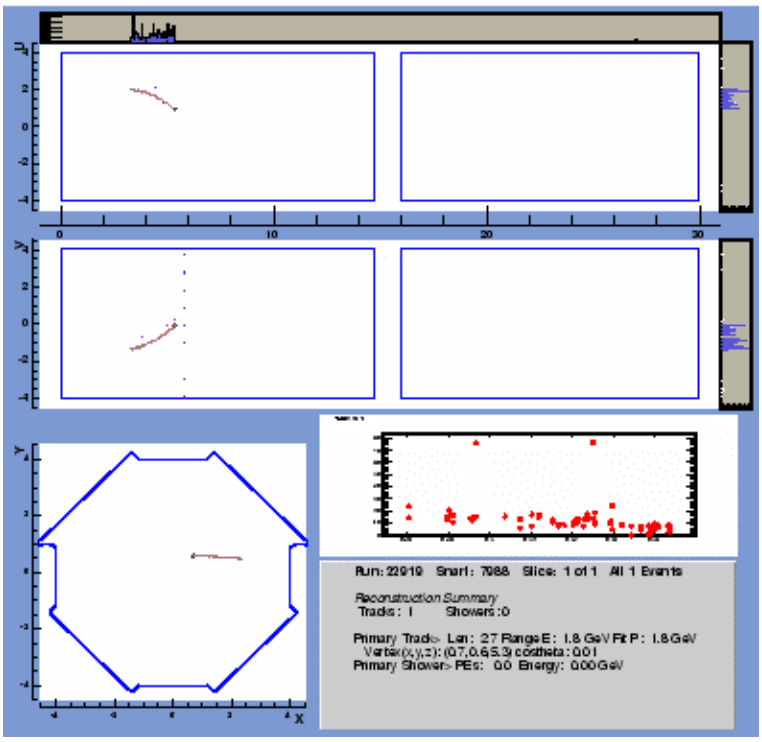

Figure 5.6 Event display for a contained neutrino event in Supermodule 1.

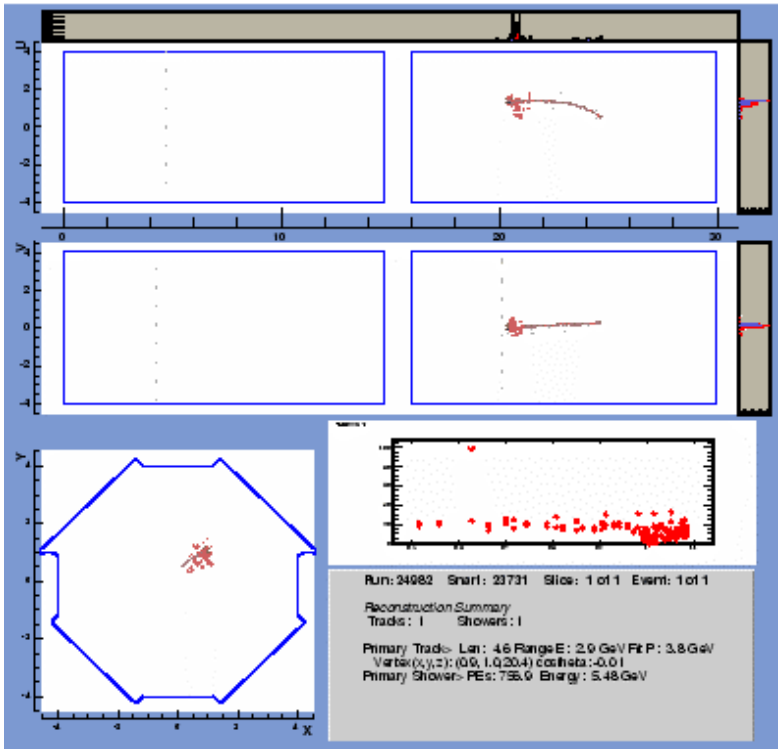

Figure 5.7 Event display for a contained neutrino event in Supermodule 2.

These events, along with other candidate neutrino events in the data set, demonstrate that both supermodules of the MINOS far detector are sensitive to atmospheric neutrinos.

5.5 Summary

The data presented in this section demonstrate that the MINOS Far Detector is capable of observing cosmic ray muon events and cosmic ray neutrino events. These events are read out through the MINOS DAQ system. They also show that all of the detector's 484 active planes are sensitive to muons. Thus, this commissioning goal has been achieved.

6 Neutrino Flux in the MINOS Near Detector

The NuMI beam produces a flux of neutrinos, some of which interact in the MINOS Near Detector. The commissioning goal requires the detection of these neutrinos.

During the NuMI commissioning run, charged-current neutrino events were generated in the target region of the MINOS Near Detector. Reconstruction of these events shows them to have momentum in the beam direction and to occur in time with the beam pulse, thus tagging them as beam-produced. The charged-current interaction rate is indicative of the neutrino flux.

6.1 Reconstruction of Charged-Current Events

Figure 6.1 is a Near Detector event display, which shows an event collected during the NuMI commissioning run on January 21, 2005. The absence of hits in the upstream planes indicates that the interacting particle is neutral. The length of the penetrating track identifies it as a muon with momentum in the beam direction. Thus, this event is identified as a charged-current interaction from a beam-produced muon neutrino.

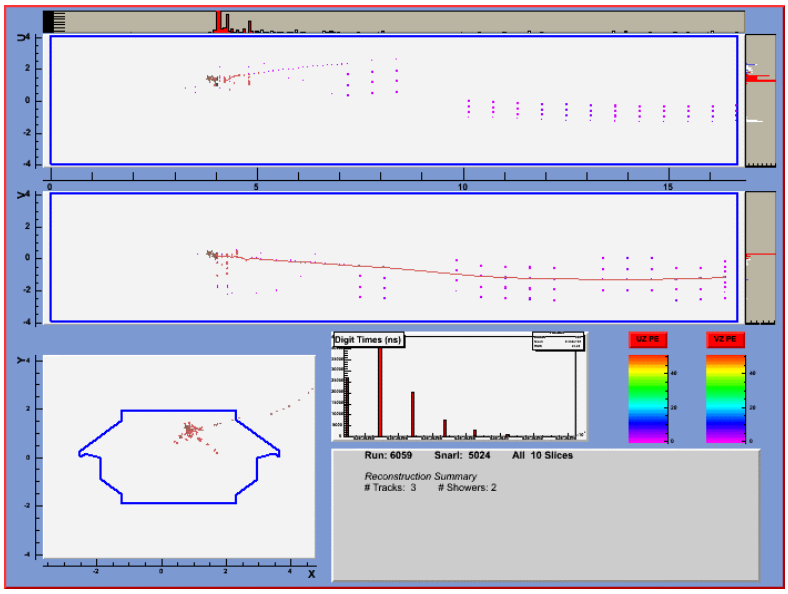

Figure 6.1 Event display of a charged-current event in the MINOS Near Detector.

Consideration of the angular distribution and timing of the candidate events demonstrates that they were produced by the NuMI beam.

6.1.1 Angular Distribution of Near Detector Events

Beam-induced events in the Near Detector will have momentum in the general direction of the beam. Figure 6.2 shows the distribution of azimuth angle and zenith angle for data taken during the commissioning run, superimposed on the distributions from cosmic rays. The red histograms are candidate neutrino events only, the black histograms are candidate neutrino events plus rock muons (muons produced by neutrino interactions in the rock upstream) and the dotted histograms are cosmic rays. The left-hand plot shows the distribution of zenith track angles. Since the beam center passes through the Near Detector at a downward angle of 3.3°, one would expect a typical cos θ value of approximately 0.06, which is consistent with the data. The right-hand plot shows the azimuth angle distribution for the same events. The expected azimuth for the beam direction is 154°. The neutrino and muon distributions are clearly peaked in the beam direction. Both the zenith and azimuthal angle distributions are markedly different from those induced by cosmic rays, demonstrating that these are beam-induced events.

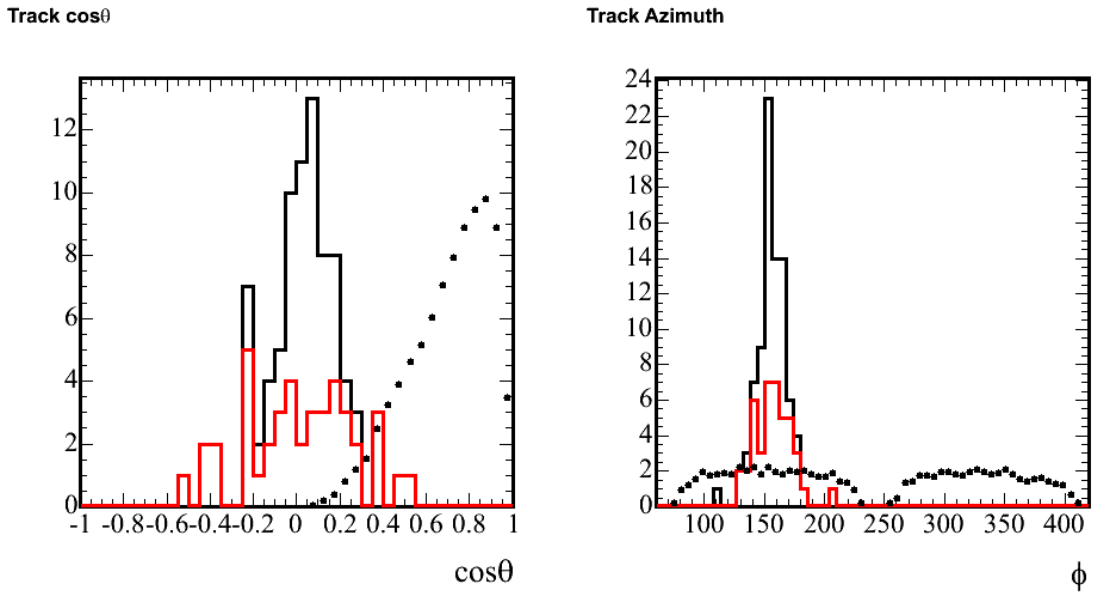

Figure 6.2 Angular distributions of neutrino candidate events from the NuMI commissioning run.

Figure 6.3 shows the distribution of the angle of event tracks with respect to the calculated neutrino beam direction. The data include both neutrino candidates and rock muons. The data collected during the commissioning run are compared with the predictions of Monte Carlo simulations run in the commissioning configuration, described in Section 7. The distribution is, to within the errors, what would be expected.

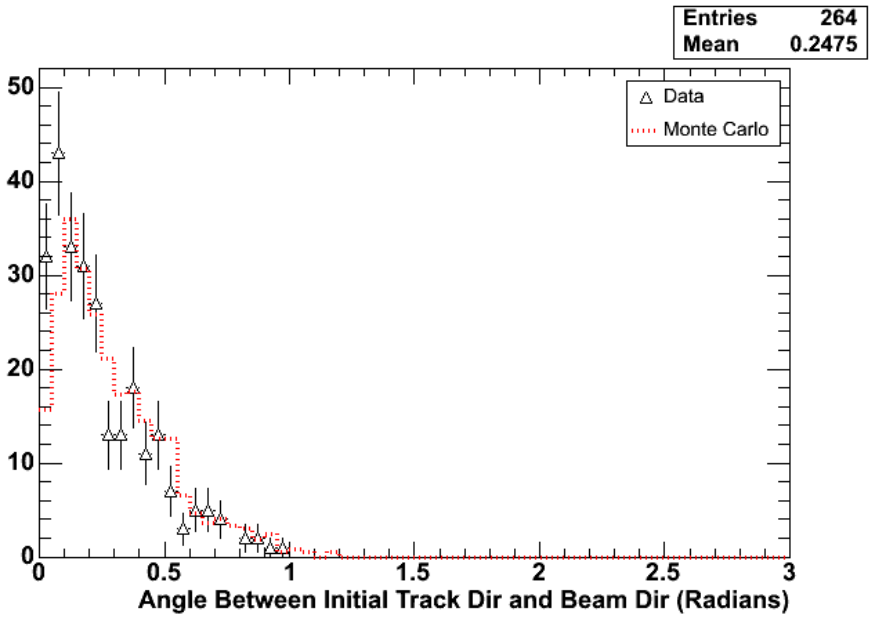

Figure 6.3 Distribution of track deviation (including rock muons) from beam angle. Data are compared with Monte Carlo predictions for the neutrino beam in the commissioning configuration.

6.1.2 Timing of Near-Detector Events

The Near Detector collected data using a beam gate for a portion of the NuMI commissioning run. The gate opened approximately 2 μs before the anticipated start of the beam spill and remained open for a period of 18 μs. During this time, all data above a specified noise threshold were read out from the detector. Figure 6.4 shows the time distribution of energy in the detector, relative to the start of the beam gate, for a total of 178 beam spills over 3 hours. The figure shows a low level of noise throughout the gate. The 1.6 μs beam spill is clearly seen as the enhancement of energy from 2 μs to 3.6 μs. All observed neutrino and rock muon events in the detector occur during this time. The small tail of energy visible for about 1 μs after the end of the beam spill is likely due to neutrons produced in neutrino interactions.

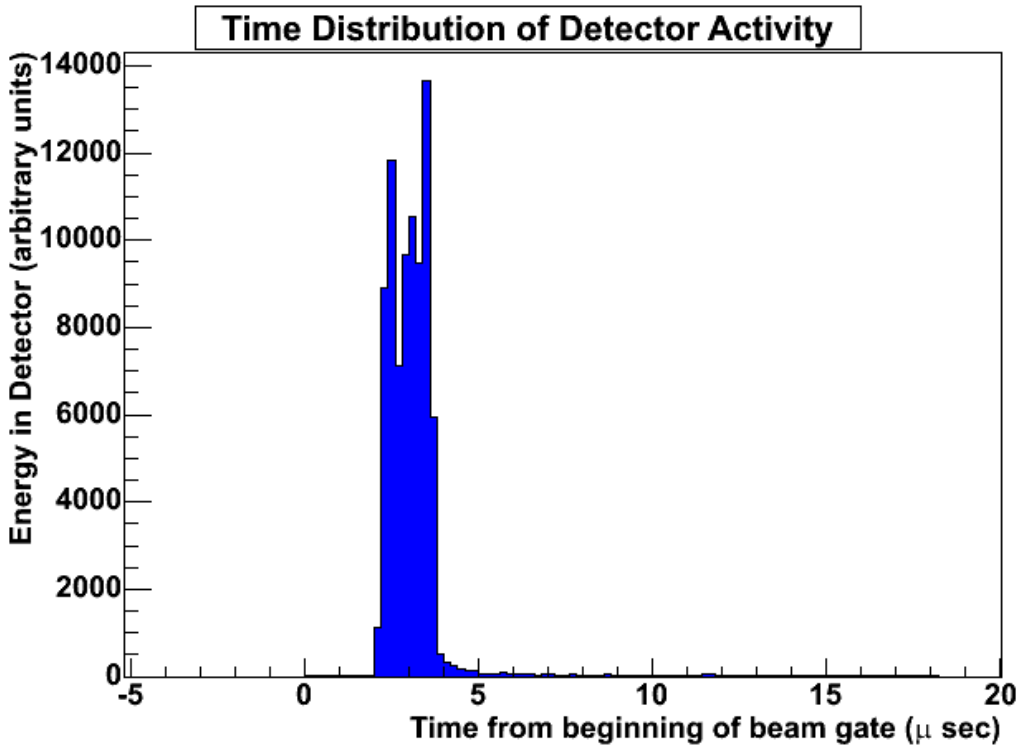

Figure 6.4 Timing plot shows the Near Detector's ADC output *vs.* time.

6.2 Charged-Current Event Rate in the MINOS Near Detector

During the NuMI commissioning run, five hours of data were recorded with the proton beam centered on the NuMI production target. A total of 8.1×10^{14} protons were delivered during this time, during which 49 charged-current neutrino events were observed in a 50-ton fiducial volume. The fiducial volume is defined to be a cylinder extending from 1 m downstream of the front face of the detector to 1 m upstream of the end of the calorimeter, 1 m in radius, centered on the intersection of the beam center line with the front face of the detector. As trigger and reconstruction efficiencies are not yet determined it is not possible to state an absolute charged-current event rate. The analysis to determine these efficiencies is presently underway.

6.3 Summary

Both neutrino and rock muon events were observed in the MINOS Near Detector during the commissioning run. The angular distributions and timing of these events demonstrates that they were induced by the NuMI beam. The number of charged-current events observed in the MINOS Near Detector with the beam in the commissioning configuration is consistent with expectations.

7 Neutrino Beam Energy

The commissioning goal is to produce neutrinos with the beamline in the low energy configuration. Such neutrinos typically have energies in the 2-4 GeV range.

In the NuMI beamline, the locations of the horns can be adjusted with respect to the target location to change the energy profile of the beam. The NuMI beam is presently in a "low energy" configuration, that is, with a low-energy beam target in place and the horns in the proper spacing for the NuMI low energy beam. The current run plan for MINOS is to spend the majority of the run time in the low energy configuration, which is designed to maximize the neutrino flux in the energy region where the expected oscillation probability is highest. Within a given horn configuration, the positioning of the target offers an additional degree of freedom. During the commissioning of the beamline, data were taken with the target pulled back 1 m relative to the normal low energy position. This "pseudo-medium energy" variant of the low energy configuration provides an increase in the overall neutrino flux. The distribution of the energies of the muons from charged-current neutrinos observed during the commissioning run is correlated to the neutrino energies.

7.1 Muon Track Energy

The energy of a muon from a charged-current interaction can be determined from the range, based on the amount of material the muon passed through before stopping. Figure 7.1 shows the energy for fully-contained tracks in the Near Detector. The kinetic energy is deduced from the amount of material through which the track passed. The selected events met a track-length criterion (42 planes) to ensure a minimum energy of 1.5 GeV. The dashed line shows the predicted muon track energy spectrum for beam events. The energies observed in the data are in good agreement with the prediction.

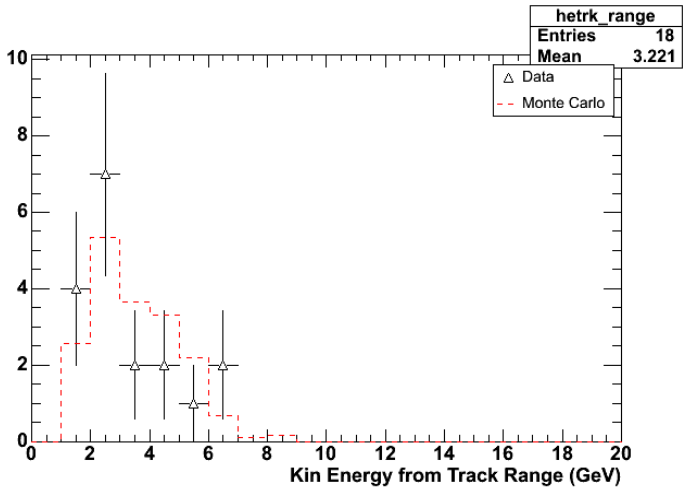

Figure 7.1 Distribution of muon energies in charged-current events determined by muon range. Data taken during the commissioning run are compared to Monte Carlo predictions for the NuMI beam in the commissioning configuration.

7.2 Summary

The muon energy distribution and the neutrino energy distribution that it implies demonstrate that the NuMI beam produces neutrinos in the energy range for which it is configured. The energy configuration will be adapted to the region in which neutrino oscillations are most likely to occur for the operational phase of the MINOS experiment.

8 Conclusion

The preceding sections of this document have presented supporting evidence for the successful completion of the NuMI Project. The NuMI Project has achieved its commissioning goals as stated in Table 1.1 and is now ready to request CD-4 from the Department of Energy. Upon obtaining CD-4 the NuMI facility and the MINOS experiment are prepared to enter their operational phase.